Nanoparticle Formation and Zeolite Growth in TEOS/Organocation/Water Solutions

Chil-Hung Cheng and Daniel F. Shantz*

Department of Chemical Engineering, Texas A&M University, College Station, Texas 77843-3122

Received: January 14, 2005; In Final Form: February 13, 2005

This work investigates nanoparticle formation and zeolite growth in several tetraethyl orthosilicate (TEOS)/organocation/water solutions heated at 368 K using small-angle X-ray scattering. The effect of several synthesis parameters including organocation identity, hydroxide content, alkali content, synthesis temperature, ethanol content, and seeding are investigated. In all cases the TEOS/organocation/water solutions lead to colloidal silica nanoparticles both after aging at room temperature and after hydrothermal treatment. In addition, the size, number density, and shape of the colloidal particles depend on the organocation identity. However, in contrast to TEOS/TPAOH/water mixtures that rapidly form silicalite-1 at 368 K, none of the investigated solutions can direct the formation of a zeolite phase at 368 K. The key point that emerges from this investigation is that it is not straightforward to synthesize siliceous zeolites from clear solutions at 368 K with the investigated organocations under the conditions where silicalite-1 forms in a matter of hours. These results suggest that the zeolite community may wish to take pause before formulating a "general" description of zeolite nucleation and growth from the studies of silicalite-1 grown from clear solution at 368 K.

Introduction

Given the importance of zeolitic materials in catalysis, adsorption, and ion-exchange processes, there is tremendous interest in developing a molecular description of their nucleation and growth.[1−4] This interest is driven by the desire to understand the fundamental science behind the material formation, as well as by the practical aspect that if one understood this process then it should open numerous avenues for both the synthesis of new materials by design and the rational property control of existing materials through synthesis. However, despite numerous efforts over the past 20 years using techniques including small-angle scattering, electron microscopy, and various spectroscopic methods (IR, Raman, NMR), this understanding has remained elusive, particularly for high-silica zeolites.[5−24] This is due to many factors: zeolites are typically synthesized at high temperatures (>400 K) where studying material formation in situ is challenging, the fundamental silicate chemistry at these conditions is poorly understood, and the mixtures contain several components.

These points have motivated the numerous studies of zeolite silicalite-1 from so-called "clear solutions" at relatively low temperatures (<373 K).[4,8,25−44] Those studies have employed both in situ and ex situ techniques including calorimetry, X-ray and light scattering, and NMR spectroscopy. The low synthesis temperature and optically transparent nature of the initial solution facilitate in situ studies, particularly those employing light scattering. The synthesis also enjoys the advantage that it is comprised of only three reagents: an alkoxysilane, typically tetraethyl orthosilicate (TEOS), tetrapropylammonium hydroxide (TPAOH), and water. As such this would appear to be as "simple" a system as one could employ to form siliceous zeolites. These points have led to numerous studies of this mixture with the hopes that a fundamental description of zeolite nucleation and growth would emerge. While there is still contention regarding the detailed mechanism of material nucleation and formation,[41,45−48] the following points are widely agreed upon: (1) after aging this mixture at room temperature small colloidal silica particles (<5 nm) are present,[26,30,35,41,43,49] and (2) after heating this mixture at 368 K for several hours small (<100 nm) particles of silicalite-1 are formed, which by all accounts nucleate homogeneously.[26−28,30] The mechanistic details of this process are still a matter of considerable debate and are the focus of numerous recent and ongoing investigations.

Despite the considerable inroads made toward understanding nucleation based on the results of these studies, the following question has yet to be posed: *How generally applicable will the results of the silicalite-1 studies be to the formation of high-silica zeolites*? This is the question addressed in this paper. We describe here a thorough investigation of nanoparticle formation and (a lack) of zeolite growth from TEOS/organocation/water solutions at 368 K of comparable composition to the clear solution synthesis of silicalite-1 ($1TEOS:0.36R^{n+}[OH^-]_n:20H_2O$). The behavior of this mixture when R is tetrapropylammonium cations has been studied extensively, so a direct comparison between the behavior of the silicalite-1 system and current work is possible. Organocations used to make ZSM-12 (MTW topology) were initially chosen since it is another pure-silica zeolite material that can be synthesized using a variety of organocations and reaction conditions.[50−61] Several synthesis parameters including organocation identity, hydroxide content, alkali content, synthesis temperature, ethanol content, and seeding have been studied. The results presented below show that the solutions studied here behave dramatically differently from TEOS/TPAOH/water solutions in their ability to nucleate and grow a zeolite phase; however, all solutions studied form stable suspensions of silica nanoparticles.

Experimental Section

Organocation Synthesis. Figure 1 shows the various organocations used in this work. Benzyltrimethylammonium hydroxide (40 wt % in water, Aldrich) and tetraethylammonium hydroxide (35 wt %, Fluka) were used as received. *N*,*N*-Diethyl-3,5-*cis*-dimethylpiperidinium iodide, *N*,*N*,*N*-trimethyl-1-ada-

* Corresponding author. Phone: (979) 845-3492. Fax: (979) 845-6446. E-mail: Shantz@che.tamu.edu.

10.1021/jp050262t CCC: $30.25
Published on Web 03/25/2005

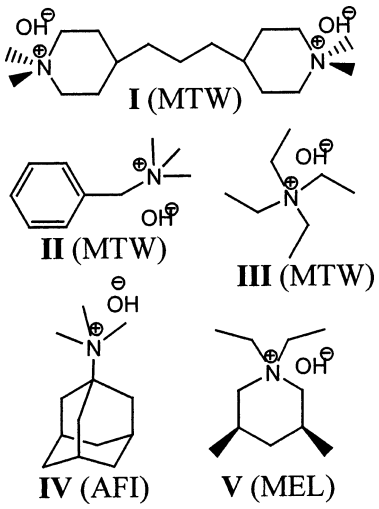

Figure 1. Organocations used in the current work.

mantammonium iodide, and 4,4′-trimethylenebis(1,1′-dimethylpiperidinium) diiodide were made using published procedures.[61,62] As an example of the synthesis of **I**, 13 mL of 4,4′-trimethylenebis(*N*-methylpiperidine) (0.05 mol, Aldrich, 98%) was mixed with 200 mL of acetone (EMD, ACS reagent). A 12 mL volume of iodomethane (0.2 mol, Aldrich, 99%) was mixed with 100 mL of acetone and transferred to an addition funnel. The iodomethane solution was added to the 4,4′-trimethylenebis(*N*-methylpiperidine) solution dropwise in the absence of light under room temperature while stirring, and the resulting mixture was allowed to react for 24 h. The white solids formed were collected by filtration and rinsed with copious quantities of acetone and dried. The crude iodide salt was recrystallized in hot methanol. The recrystallized salt was ion-exchanged twice by using 5-fold excess ion-exchange resin (IONAC NA38, OH^- Form Type L Beads, J. T. Baker). The resulting 4,4′-trimethylenebis(1,1′-dimethylpiperidinium) dihydroxide solution was concentrated by rotary evaporation at 120 mbar and 333 K. The ion-exchange efficiency and the concentration of the organocation solution were determined by titration with 0.16 N HCl solution using Cresol red (Aldrich, indicator grade, 95%) as an indicator. The exchange efficiency was greater than 95%, and the organocation solution was concentrated to approximately 20−30 wt %.

Zeolite Synthesis. Syntheses were typically of the composition $1TEOS:0.36/nR^{n+}[OH^-]_n:20H_2O$; the exact compositions are denoted in the figures and text. The following general procedure was followed: 9.2 mL of tetraethyl orthosilicate (Fluka, >99%) was added to the organocation solution, typically 20−40 wt % organic (**I**−**V**). This mixture was stirred vigorously for 1 h, and any additional water needed was then added. The solution was then aged for 24 h while mixing at room temperature. The solution was then placed in a screw-cap Teflon container and heated at 368 K for the designated period of time. Syntheses performed at higher temperatures (393−433 K) were performed in 23 mL Teflon-lined Parr autoclaves. A comparative synthesis was also performed where the ethanol generated by the hydrolysis of the TEOS was removed using a high vacuum manifold system under room temperature. The ethanol and water mixture was trapped by liquid nitrogen. This step was sustained until half the solution volume was left. Additional water was subsequently added to make up the water lost during the evaporation. Heated samples were quenched in an ice bath prior to SAXS measurements or nanoparticle extraction. ZSM-12 seeds were made as described previously[61] from a mixture of composition $1SiO_2:0.06$**I**$:0.3NaOH:32H_2O$ heated statically at 433 K for 14 days.

Nanoparticle Extraction. The extraction procedure followed was similar to that described by Schoeman.[28] A 27 mL volume of the ZSM-12 solution was added to 70 mL of 0.5 N HCl and stirred for 30 min. All solutions were cooled in an ice bath prior to mixing. Then, 60 mL of tetrahydrofuran (THF; EMD, >99%) was added to the acidified ZSM-12 solution and stirred for another 30 min. Finally, 15 g of NaCl (EMD, >99.5%) was added to the above mixture and stirred for another 30 min. The solution separated into two layers by the end of this treatment. The aqueous layer was removed by using a separatory funnel, the organic layer, containing the nanoparticles, was collected, and the THF was removed by rotary evaporation under reduced pressure at 333 K. The resulting opaque solution was then decanted and dried in a Petri dish. The dried solids were then ground with a mortar and pestle before further characterization. To wash the solids, 200 mg of grounded solids was resuspended in 25 mL of deionized water and centrifuged at 3000 rpm for 15 min. The supernatant was decanted, and the residual solids were rinsed with 25 mL of fresh deionized water for centrifugation. The procedure was repeated four times. The rinsed powders were dried at room temperature for 2 days.

Analysis. Powder X-ray diffraction (PXRD) measurements were performed using a Bruker-AXS D8 powder diffractometer (Cu Kα radiation) in reflection mode at $2\theta = 4-40°$ with a step size of 0.03° and 2 s per step. Fourier transform infrared (FTIR) measurements were performed using a Nicolet 720 spectrometer. Samples of 5 mg were mixed with 500 mg of KBr (Aldrich, > 99%) and pressed into pellets. The measuring chamber was degassed prior to the background and sample measurements. The spectra were collected in transmittance mode from 400 to 4000 cm^{-1}. Thermogravimetric analyses (TGA) were performed using a Universal TA instrument (Q500 v5.3) with a heating rate of 5 K/min from room temperature to 873 K under air environment. The air flow rate was 15 mL/min. Dynamic light scattering measurements were performed using a BIC ZetaPALS at room temperature using a quartz cuvette (Starna Cell Co., 1-Q-10-GL 14-C). The wavelength of the incident laser beam was 658 nm. The detecting angle was 90°. The organocation solution was filtered using a 0.2 μm PES syringe filter (Corning Co.) prior to loading into the quartz cuvette in order to eliminate any dust. For each sample, three measurements were performed and the running time of each measurement was 5 min to ensure high signal-to-noise ratio and good counting statistics. The autocorrelation functions were analyzed with the double-exponential method.[63] The viscosity of each sample was measured using an Ubbelohde-type viscometer (0C, Cannon Instrument Co.). The viscous constant of the viscometer was 0.003 cSt/s.

Small-angle X-ray scattering experiments were performed using a Bruker NanoSTAR system with a Nonius rotating anode (FR591) and a copper target (1.5417 Å). The anode was operated at 45 kV and 90 mA. The X-ray beam was paralleled by a cross-coupled Göbel mirror and collimated by three pinholes (750, 400, and 1000 μm in order). The scattering intensity was measured on a two-dimensional multiwire Hi-STAR detector, and the residual direct beam was blocked by a beam stop. The whole system was operated under vacuum (10^{-2} mbar). The detector was located 22 and 64 cm away from the sample, corresponding to a q range of 0.05−0.7 and 0.02−0.3 $Å^{-1}$, respectively ($q = 4\pi \sin(\theta)/\lambda$; θ is half the scattering angle and λ is the wavelength of the incident beam). The exact sample-to-detector distance was determined using a silver behenate

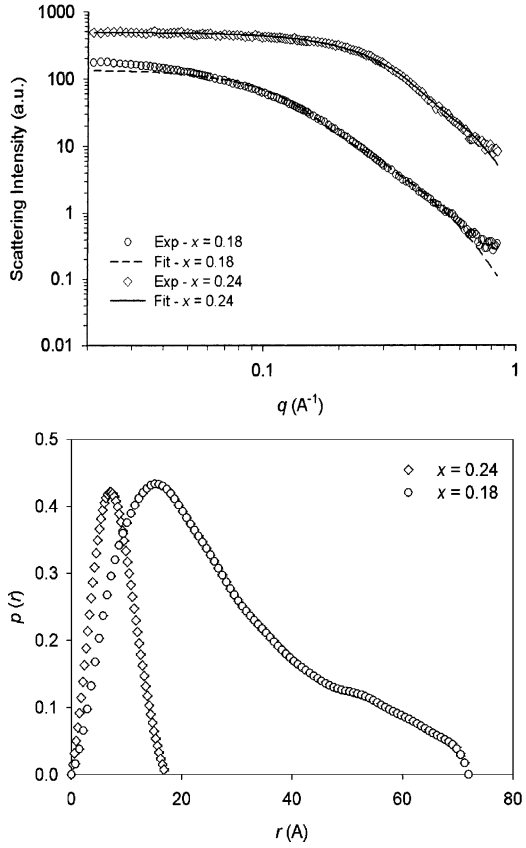

Figure 2. (top) SAXS data and full profile fit for mixtures 1TEOS:*x***I**:20H_2O aged for 24 h at RT. (bottom) Corresponding pair distance distribution functions.

standard. The zeolite precursor solution was loaded into a 1-mm-diameter Anton Paar quartz capillary and mounted in an Anton Paar HR-PHK sample chamber. A computer-controlled step motor connected to the sample stage was used to position the sample in the path of the incident beam. For obtaining the transmission coefficient of the sample, a piece of glassy carbon was inserted into the beam path as a second specimen after each measurement. Because of the pinhole collimination system, no desmearing of the data is necessary. The scattered intensity of the particles was calculated based on using water as the reference material for the background subtraction in data analysis.[9,12] The scattering data were analyzed using the program GNOM to determine the pair distance distribution function (PDDF) using the inverse Fourier transform method.[64−68] Full profile fitting was also performed using a least-squares method described by Pederson.[69]

Results

Solutions with 4,4′-Trimethylenebis(1,1′-dimethylpiperidinium) Dihydroxide (I). The initial goal of this study was to investigate the nucleation behavior of ZSM-12 from clear solutions analogous to those from which silicalite-1 can be formed. **I** was chosen because it can be used to make ZSM-12 over a reasonably broad Si/Al range (Si/Al $\sim$ 30−∞) and with varying alkali contents.[57,58,60,70] Optically transparent homogeneous solutions were obtained from mixtures of composition 1TEOS:*x***I**:20H_2O (x = 0.12, 0.18, and 0.24) aged at room temperature (RT) for 24 h. Figure 2 shows the SAXS patterns, results of full profile fitting, and pair distance distribution function (PDDF, $p(r)$) of the mixtures aged for 24 h at room temperature. The appearance of a plateau in the scattering pattern at low q range indicates that particles above approximately 20 nm in diameter are not present, and the lack of a clear maximum at intermediate q range suggests that the structure factor ($S(q)$) due to particle−particle interactions is not significant.[69,71] The absence of larger particles in these mixtures was further verified using dynamic light scattering (DLS; Supporting Information). The scattering data in the low q range can be used to estimate the particle radius of gyration using Guinier analysis,[72] which is 20 and 7 Å for the mixtures with x = 0.18 and 0.24, respectively. In both cases the slope in the high q range is −2.7. The full profile fitting of the scattering pattern using a variety of particle geometries (spheres, cylinders, concentric sphere, and ellipsoids) indicates the best fit of the experimental data is the case of ellipsoidal particles based on the χ^2 values (see Supporting Information). The PDDF for the x = 0.18 sample is comparable to what one would expect from ellipsoidal particles; however, the feature at higher r values is not adequately described by the fit. Two sources of discrepancy exist: the tail is due to either particle−particle interactions (i.e., structure factor effects) or polydispersity. Full profile fitting assuming a bimodal population of ellipsoids yielded a best fit of R = 16 and 5 Å for the two populations. This, however, still could not account for the features at high r values (Supporting Information). Given that to the best of our knowledge analytical structure factor expressions do not exist for ellipsoidal scatterers, this could not be included in the full profile fitting. A clear maximum is not observed in the I versus q plot, but based on the analysis above, particle−particle interactions cannot be ruled out. Moreover, given the ambiguity in introducing polydispersity for nonspherical particles (i.e., polydispersity in one or two directions and the subsequent increase in fitting parameters), subsequent fits are shown only for monodisperse particles, ignoring polydispersity effects. This was chosen to keep the fits relatively simple, yet still capturing (at least qualitatively) the trends in particle size. The fits yield primary axis values of R = 23, 23, and 4 Å and R = 9, 9, and 3 Å for the mixtures with x = 0.18 and 0.24 individually. The fit for triaxial ellipsoids gives comparable results, and as such it is more appropriate to use the biaxial model because it has fewer parameters. The pair distance distribution functions are consistent with the results of the full profile fitting. Table 1 summarizes the scattering results of the samples aged at room temperature before heating. The size of the particles depends on the pH, which varies with the organocation content, as would be expected.[25]

The mixtures with x = 0.12 gelled after heating at 368 K for 1 day while the other two mixtures remained transparent homogeneous solutions during hydrothermal reaction. The samples discussed here have been heated for 2 weeks; however, syntheses of composition 1TEOS:0.18**I**:20H_2O have been left to react over several months and this mixture remains optically transparent. That no trace of solid zeolite phase could be observed suggests an extremely slow nucleation/crystallization rate or the complete absence of crystallization in these solutions. Figure 3 shows the SAXS patterns, results of full profile fitting, and pair distance distribution functions of the heated mixtures. The scattering patterns of the heated samples also have a plateau in the low q range within the examined q range, which indicates that no larger particles were formed in the ZSM-12 precursor solutions during hydrothermal reaction. The SAXS patterns of the mixtures heated for only 1 week (Supporting Information) appear nearly identical to those heated for 2 weeks. The slope in the high q range is again approximately −2.7. The full profile fitting of the scattering pattern indicates the particles are ellipsoidal with primary axis values of R = 16, 16, and 4 Å and R = 12, 12, and 3 Å for the mixtures with x = 0.18 and

TABLE 1: Summary of SAXS Fitting of Mixture 1TEOS:*x*I:20H_2O as a Function of Synthesis Duration[a−c]

	particle shape, size (full profile fitting)				particle shape, size (PDDF)		particle dimensions by Guinier analysis	
	$x = 0.18$		$x = 0.24$					
t, days	R	ϵ	R	ϵ	$x = 0.18$	$x = 0.24$	$x = 0.18$	$x = 0.24$
0	23	0.15	9	0.30	22	9	20	8
7	20	0.10	9	0.27	7	10	9	7
14	16	0.19	12	0.20	9	9	9	8

[a] Sizes are given in angstroms. [b] The results of the fit are for monodisperse biaxial ellipsoids. [c] The form factor amplitude of a biaxial ellipsoid of dimensions *R*, *R*, ϵ is given by the following equations,

$$P(q,\epsilon,R) = \int_0^{\pi/2} \left\{ \frac{3[\sin(qR_{ellip}) - (qR_{ellip})\cdot\cos(qR_{ellip})]}{(qR_{ellip})^2} \right\}^2 \cdot \sin(\alpha)\, d\alpha$$

$$R_{ellip} = R[\sin^2(\alpha) + \epsilon^2\cdot\cos^2(\alpha)]^{1/2}$$

where *R* is radius of the ellipsoid; ϵ is the aspect ratio; and *q* is the scattering vector.

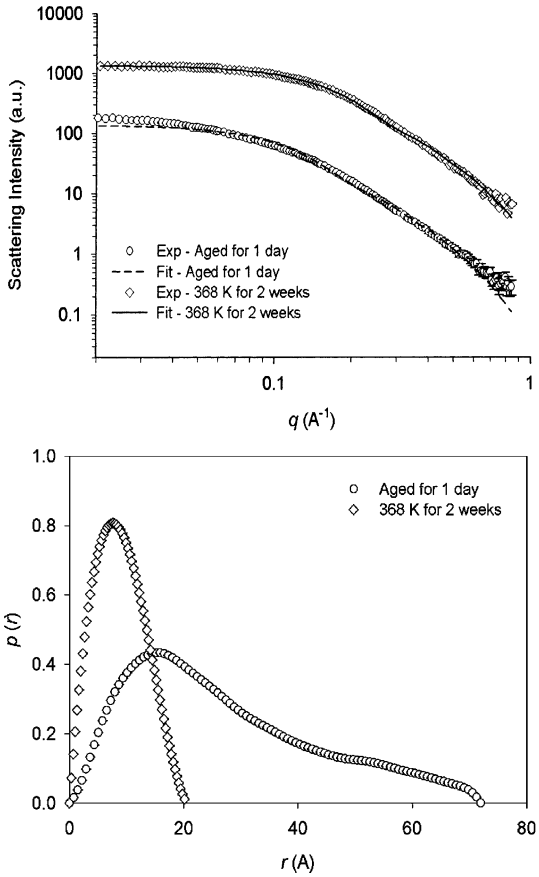

Figure 3. (top) SAXS data and full profile fit for mixtures 1TEOS: 0.18**I**:20H_2O after aging at RT and heating for 2 weeks. (bottom) Corresponding pair distance distribution functions.

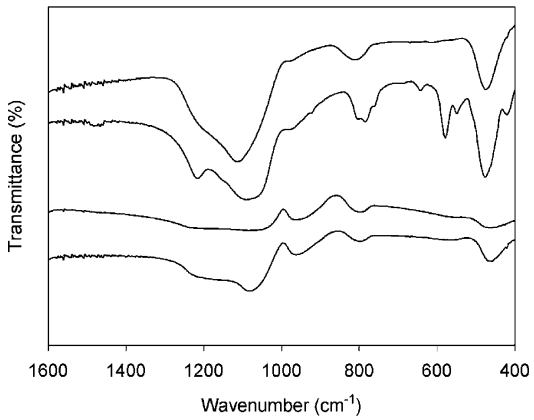

Figure 4. Infrared spectroscopic data of particles extracted from the mixture 1TEOS:0.18**I**:20H_2O after (from bottom to top) aging at RT, 1TEOS:0.18**I**:20H_2O after heating for 2 weeks at 368 K, ZSM-12, and Cab-O-Sil.

0.24, consistent with the pair distance distribution functions. Table 1 summarizes the scattering results of the mixture 1TEOS: 0.18**I**:20H_2O as a function of the synthesis duration. Perhaps most significant is that the particles in the mixture 1TEOS:0.18**I**: 20H_2O *decrease* in size once the mixture is heated; this is interpreted to mean the larger ellipsoidal particles observed after room temperature aging decrease in size, yielding a narrower size distribution. By contrast, the mixture with the highest organic content ($x = 0.24$) appears to be insensitive to heating. Both the full profile fitting and the PDDF analysis indicate that there is very little change in the size and shape of these particles over the synthesis periods investigated. Given that the current work is limited to SAXS data, i.e., small-angle neutron scattering measurements were not performed, there is some ambiguity as to the exact structure of these particles, especially given that the PDDFs of some of the fits (e.g., cylinders versus ellipsoids) are quite similar. However, it is clear that in the syntheses above no particles larger than 10 nm in size form during the course of the synthesis.

Effect of Synthesis Temperature and Alcohol. One possible explanation for the results above is that the activation energy for nucleation and/or growth is simply higher in this system than in the silicalite-1 system. To verify this, a series of experiments were performed where the synthesis temperature was varied. Syntheses performed at 418 and 433 K for 7 days with **I** ($x = 0.18$) resulted in gels that are amorphous silica based on PXRD (Supporting Information). The same mixtures yielded a layered silicate phase after being heated at 418 and 433 K for 14 days (Supporting Information). It is important to note that mixtures of composition 1TEOS:0.36TPAOH:20H_2O heated at the same temperatures and duration form highly crystalline silicalite-1 (Supporting Information). These results show that even at "conventional" synthesis temperatures ZSM-12 cannot be formed from these mixtures. This shows either that it is not possible to make ZSM-12 from these mixtures or that the kinetics of the process is extremely slow. The latter point would indicate that the activation barrier must be significant to have such a suppression of growth. Based on the well-known ability to make ZSM-12 under a wide range of mixture compositions at this temperature,[50−61] we postulate that it is not possible to make ZSM-12 from mixtures of this composition.

The effect of the alcohol content was also studied by performing syntheses where the ethanol generated by the

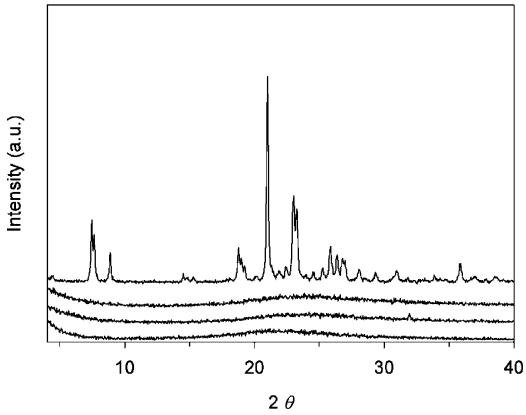

Figure 5. Powder X-ray diffraction patterns of samples (from bottom to top): Cab-O-Sil, mixtures 1TEOS:*x*I:20H_2O ($x = 0.18$, 0.24) after 2 weeks at 368 K, and ZSM-12.

hydrolysis of TEOS was removed before hydrothermal treatment. This mixture, upon heating at 368 K for 2 weeks, also yielded small (<20 nm) particles and did not crystallize the MTW phase (Supporting Information). Given that the goal of this study was to investigate the formation of other zeolite phases from TEOS/organocation/water mixtures similar to those used to make silicalite-1, other silica sources were not investigated. The effect of the organocation identity, and of the presence of alkali cations and seed crystals, has also been studied. Before turning to those results, however, some characterization results of solids extracted from the above mixtures will be described.

Thermogravimetric Analysis (TGA)/FTIR on Extracted Particles. As a comparison to the numerous studies of materials extracted from silicalite-1 syntheses,[35,37,41] included here are TGA, IR, and PXRD results on solids extracted from the above mixtures. From the differential weight loss curve in TGA measurements, there exists one obvious weight loss event at approximately 353 K and two minor weight losses occurring above 373 K. The weight loss peak around 353 K is due to desorption of physically adsorbed water.[41] The weight loss peaks above 373 K could be attributed to the decomposition or desorption of the organocation or the condensation of the silanol groups, resulting in the generation of water. The silanol groups here are likely associated with the external surface of the particles, but may also be present as siloxy groups acting as charge compensators for the organocations.[73] The TGA data can be found in the Supporting Information, but approximately 23.8 wt % loss is observed below 373 K, and typically the weight loss above 373 K is less than 6 wt %. Moreover, the weight loss decreased after the extracted solids were rerinsed with deionized water. This result shows that any organic cations that may be associated with the silica particles are on the outer surface, *not* occluded in them. As compared with the TGA measurement on the extracted silicalite-1 nanoparticles published by Kragten et al.,[41] the first minor weight loss is about 12.8 wt %, much higher than what is obtained on the solids extracted from solutions containing **I**.

The IR spectra of the as-extracted and rinsed samples are shown in Figure 4; the IR spectra of crystalline ZSM-12 and Cab-O-Sil are shown for comparison. All IR spectra of the extracted samples show a C−H stretching band at 2800 cm^{-1}, indicating that some organocations are associated with the extracted silicate particles, consistent with TGA results. All samples extracted from the clear solution syntheses appear very

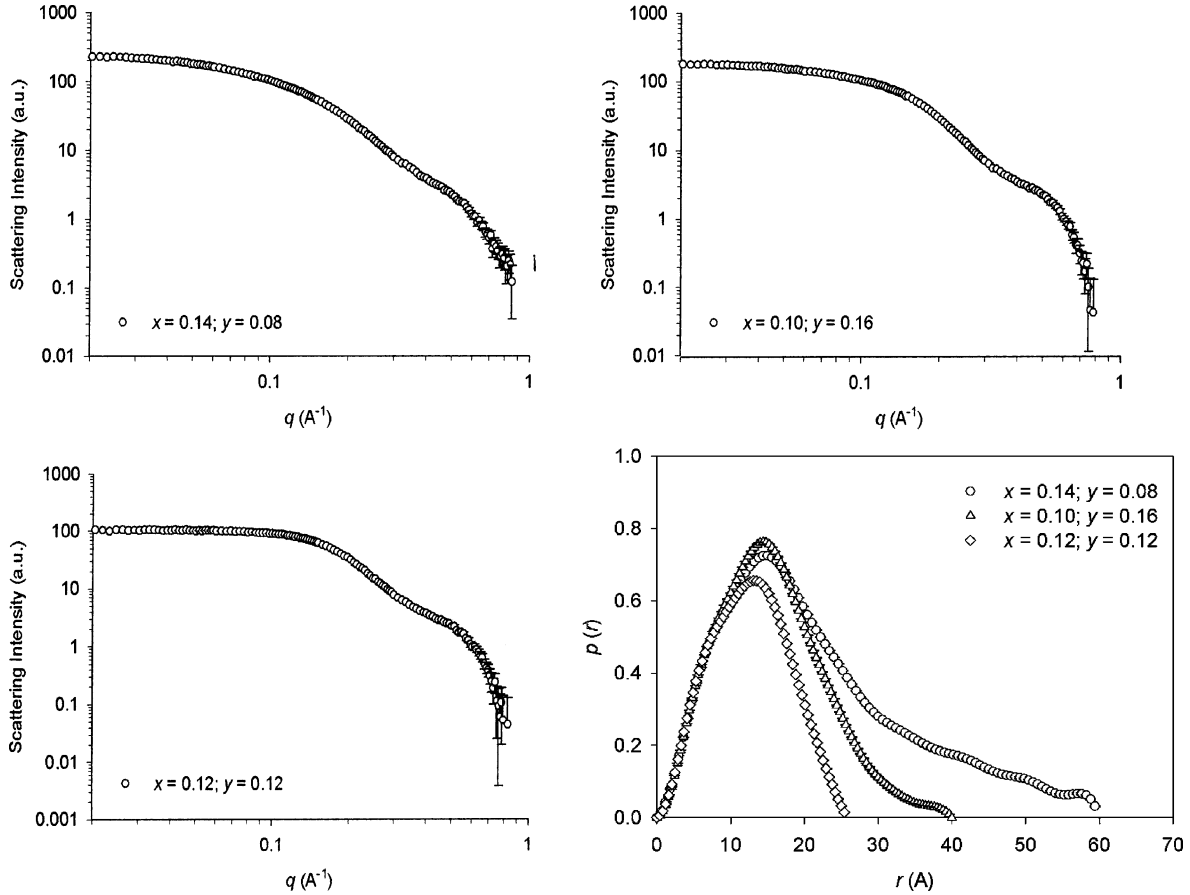

Figure 6. SAXS data for mixtures 1TEOS:*x*I:*y*NaOH:20H_2O ($2x + y = 0.36$) after heating for 2 weeks at 368 K. (bottom right) Corresponding pair distance distribution functions.

similar to amorphous silica based on the IR spectra in the region of 520−700 cm^{-1}. ZSM-12 exhibits two clear peaks at 550 and 578 cm^{-1}, assigned to double five-membered silicate rings,[74,75] which are not observed in the as-extracted and rinsed samples. For the as-extracted and rinsed samples, the IR spectra show a broad band in the interval of 520−700 cm^{-1}, very similar to the spectrum of Cab-O-Sil. The IR of the extracted materials is consistent with that of amorphous silica. A strong band in the range of 420−500 cm^{-1} appears for all the samples and is the Si−O bending mode. As shown in Figure 5, the PXRD patterns of the as-extracted and rinsed samples also show that the extracted samples are amorphous.

The work above shows that the clear solutions employed can form stable nanoparticles of silica, which appear to contain few organocations, and do not nucleate zeolite ZSM-12 upon heating. The presence of silica nanoparticles is consistent with recently published work by Fedeyko and co-workers that shows tetraalkylammonium (TAA) hydroxide solutions can stabilize colloidal silica particles.[49] The results shown above indicate this is not unique to TAA cations; the work discussed below reinforces the generality of this observation. However, it is well-known that the growth of ZSM-12 is highly sensitive to the alkali content present in the synthesis mixture.[57] With that in mind the next step was to investigate the effect of sodium content and seeding on the nucleation and growth of ZSM-12 from clear solutions.

Effect of Sodium Hydroxide and ZSM-12 Seeds. Without observing any crystallization of ZSM-12 zeolite phase from the clear precursor solution hydrothermally reacted at 368 K for 2 weeks, the effect of varying the alkali content was then studied, since it has been reported that alkali cations can strongly influence crystallization kinetics.[57] Mixtures of composition 1TEOS:x**I**:yNaOH:20H_2O were studied, where $2x + y = 0.36$, by varying the NaOH content while keeping the initial hydroxide concentration fixed. The precursor solutions were still transparent after being heated for 2 weeks at 368 K. The SAXS patterns and pair distance distribution functions of the heated mixtures are shown in Figure 6. The scattering patterns again show a plateau in the low q range, indicating that no particles greater than 20 nm are formed after heating. All attempts at full profile fitting of the data were unsatisfactory, and the tail observed at high r values in the PDDFs suggests the presence of particle−particle interactions. For all three mixtures small particles are observed, and none of the mixtures nucleate a zeolite phase. These results indicate that under these conditions the presence of sodium does not enhance the formation or growth rate of ZSM-12.

It is well-known that the addition of seed crystals can enhance the rate of zeolite formation and growth.[76] Several experiments were also performed using ZSM-12 seeds to investigate the possibility of ZSM-12 formation by seeding. These mixtures, that contain 75 mg of ZSM-12 crystals in a synthesis mixture of 27 mL, became opaque after 24 h of room temperature (RT) aging. After heating the mixtures at 368 K for less than 1 day, the solutions gelled and remained gels after 2 weeks at 368 K. The solids are amorphous silica based on PXRD (Supporting Information). These results show that (1) the seeds do not serve as a source for forming ZSM-12 particles that are <100 nm, and (2) further growth of the seeds is not observed.

Effect of Organocation Identity. Unable to synthesize ZSM-12 zeolite with **I**, the investigation shifted to other organocations, notably **II** and **III** that have also been shown to make ZSM-12.[51,58,70] In both cases the mixtures were optically transparent after aging at room temperature for 24 h and after 2 weeks at

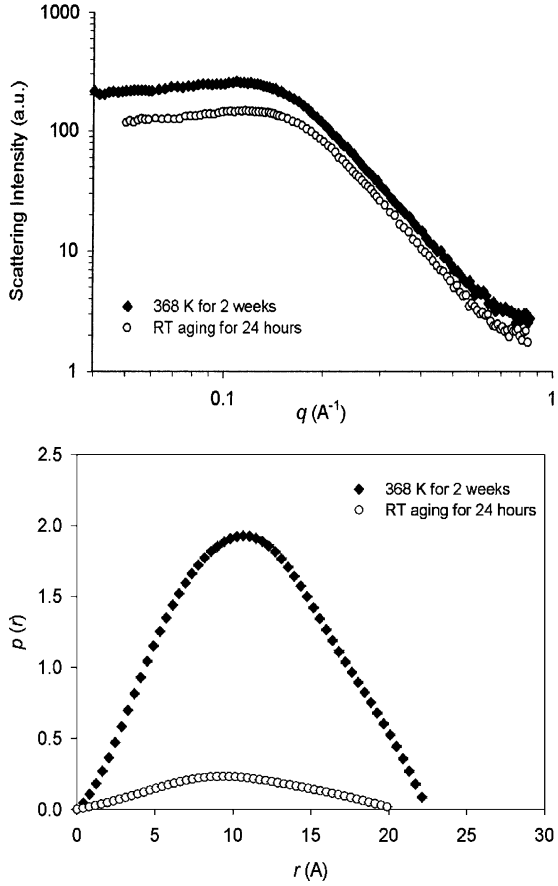

Figure 7. (top) SAXS data of mixtures 1TEOS:0.36**II**:20H_2O after aging at RT for 24 h and heating for 2 weeks. (bottom) Corresponding pair distance distribution functions.

368 K. The SAXS results for mixtures of composition 1TEOS: 0.36R^+OH^-:20H_2O after aging at room temperature and 2 weeks at 368 K are shown in Figures 7 and 8. For both samples the slope of the scattering patterns in the high q range is about −2.9. In addition, the scattering patterns of both samples display a maximum at $q \sim 0.12$ $Å^{-1}$, which is similar to silicalite-1 prepared by using tetrapropylammonium hydroxide (TPAOH) after room temperature aging.[43] Three of the four scattering curves exhibit a clear maximum in the plots of log I versus log q, consistent with the presence of structure factor effects (i.e., particle−particle interactions). Attempts to fit the scattering patterns proved unsatisfactory. The particles are not spherical based on the slope in the high q range. Given that analytical structure factor expressions are not available for most particle geometries, full profile fitting was not pursued further. Guinier analysis shows the radius of gyration to be approximately 15 Å, and PDDF analysis indicates the radii of gyration are close to each other, from 16 to 15 Å upon heating at 368 K. It is important to note the PDDF results are only qualitative as the formalism is not strictly valid once particle−particle interactions become important. The scattering patterns for both samples are qualitatively similar before and after heating. The one noticeable difference is that the maximum observed at approximately $q \sim 0.12$ $Å^{-1}$ for the aged mixture containing **III** disappears upon heating, likely due to a decrease in the number density of particles which would lead to a decrease in the particle−particle interactions that give rise to the maxima. However, in both cases the SAXS data clearly show that all particles in the samples are below 10 nm in size, again consistent with the observation that neither of these organocations can nucleate nor crystallize a zeolite phase under these conditions. The precursor solutions

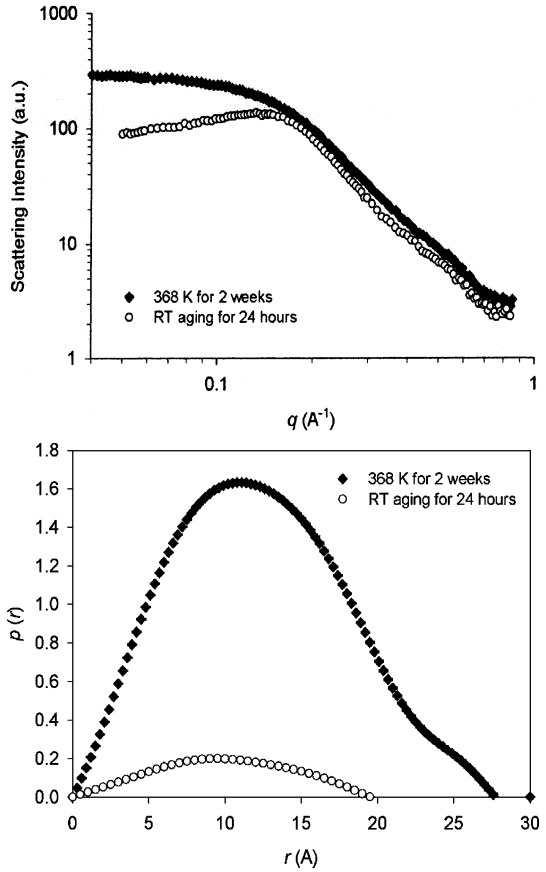

Figure 8. (top) SAXS data of mixtures 1TEOS:0.36**III**:20H_2O after aging at RT and heating for 2 weeks. (bottom) Corresponding pair distance distribution functions.

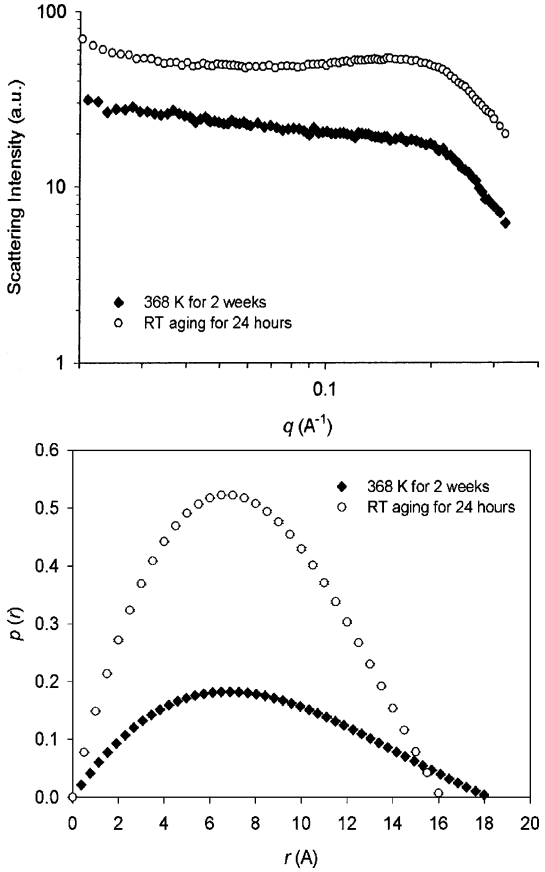

Figure 9. (top) SAXS data of mixtures 1TEOS:0.36**IV**:20H_2O after aging at RT and heating for 2 weeks. (bottom) Corresponding pair distance distribution functions.

containing **II** were also hydrothermally treated at 418 and 433 K. The mixture formed gels at 418 K for 7 days and 14 days. The solids are amorphous silica based on PXRD (Supporting Information). The same result was obtained for the mixture heated at 433 K for 7 days; however, the mixture yielded poorly crystalline material after being heated at 433 K for 14 days (Supporting Information). Given the poor crystallinity of the material and the few peaks present in the diffraction pattern (approximately six), conclusive phase identification is not possible, although all peaks can be attributed to either silicalite-1 or ZSM-12 (although not all the peaks can be attributed to one phase). Previous work by Shantz and co-workers has shown that siliceous ZSM-12 can be made with this (SDA),[77] and those syntheses employed low sodium hydroxide content.

The work above clearly shows that it is not possible to nucleate and grow ZSM-12 from solutions of similar composition that make silicalite-1 at 368 K. To assess whether this was unique to ZSM-12, syntheses were performed using **IV** and **V**. **IV** is perhaps the quintessential example of a nonselective SDA, as it can be used to make several different zeolitic materials.[17] The SAXS results for a mixture of composition 1TEOS:0.36**IV**:20H_2O after aging at room temperature and 2 weeks at 368 K are shown in Figure 9. Similar to the case of **III**, the scattering pattern of RT aging sample exhibits a maximum at $q \sim 0.2$ $Å^{-1}$ and the feature subsequently disappears after the mixture was heated for 2 weeks at 368 K. It is worth noting that the scattering pattern in the low q range displays an increasing magnitude of scattering intensity, indicating that larger particles do form in this mixture, though it remained optically transparent during the synthesis period studied here. In addition, the presence of a maximum in the scattering pattern indicates that the structure factor efforts cannot be neglected in this case. On the basis of Guinier analysis, the radii of gyration are about 36 and 47 Å for the samples that are aged at room temperature for 24 h and heated for 2 weeks at 368 K individually, which are consistent with results from GNOM. After 4 months of heating this mixture at 368 K, solids were observed. The PXRD of those solids cannot be indexed to any known phase (e.g., SSZ-24, SSZ-23, MCM-22 precursor), which appears to be a layered silicate phase. Ongoing work is characterizing this material further.

Syntheses were also performed with **V**, which has been shown to selectively nucleate pure phase ZSM-11.[62,78] Hence, **V** can be regarded as a highly selective SDA. The precursor mixtures were optically transparent after aging at room temperature for 24 h and after 2 weeks at 368 K. The SAXS scattering pattern of the room temperature aging sample, which is shown in Figure 10, also displays a maximum at $q \sim 0.2$ $Å^{-1}$, indicating that particle−particle interactions still exist in the mixture. The appearance of the feature hampers our attempt to perform full profile fitting on the scattering pattern. The slope in the high q range is about −2.5, which shows that the particles are not spherical. The scattering pattern forms a plateau in the low q range after the solution has been heated at 368 K for 2 weeks, and it is worth noting that the maximum still exists but is not obvious after 2 weeks of heating. Again given the nonspherical shape of the particles and the presence of the structure factor effects, full profile fitting was not attempted. On the basis of Guinier analysis, the radii of gyration of the particles are about 10 and 8 Å, respectively, for the sample aging at room temperature and 2 weeks at 368 K. The GNOM analysis shows similar results. The result demonstrates that the particle size

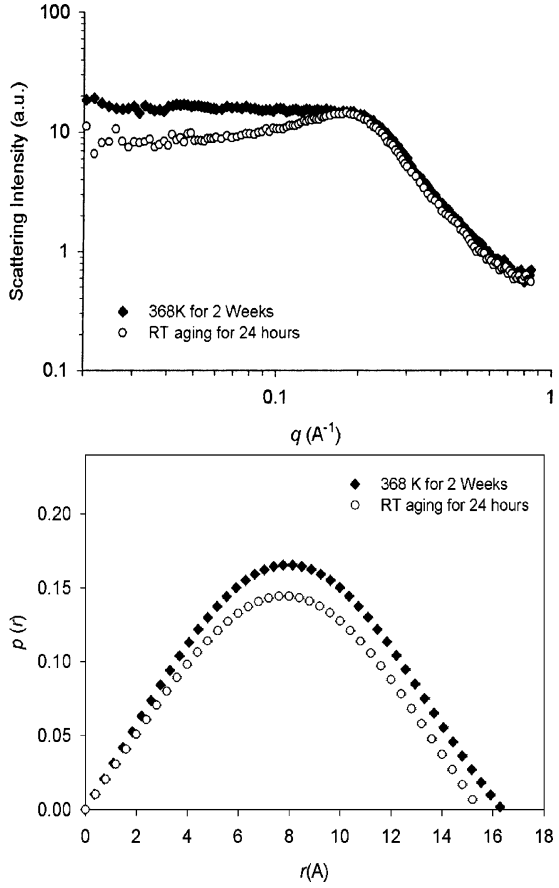

Figure 10. (top) SAXS data of mixtures 1TEOS:0.36**V**:20H_2O after aging at RT and heating for 2 weeks. (bottom) Corresponding pair distance distribution functions.

decreases and the precursor solution cannot form any zeolitic phase after the solution is heated at 368 K for 2 weeks.

Discussion

This work has investigated five different organocations of different sizes, shapes, and C/N^+ ratios. In all cases it is not possible to nucleate and crystallize a zeolite phase under conditions where silicalite-1 forms rapidly. However, in all cases silica nanoparticles are observed, and the size, shape, and number density of these particles appear to be dependent on the identity of the organocation. This observation is consistent with recent work by Fedeyko and co-workers[49] and suggests that the formation of silica nanoparticles in alkaline mixtures of quaternary ammonium cations is a general phenomenon.[79] As such it would appear from this work that while all TEOS/organocation/water solutions investigated give rise to silica nanoparticles, of the nearly 10 organocations studied between this and previous work by Fedeyko and co-workers only TPAOH can direct zeolite nucleation and growth at 368 K. As a control, a solution of 1TEOS:0.36TPAOH:20H_2O was also heated at 368 K and studied with SAXS (Supporting Information). Consistent with all previous literature, this mixture rapidly leads to the formation of silicalite-1. That the different organocations give rise to suspensions containing nanoparticles of different sizes, shapes, and number densities suggests new possibilities for using these particles in solution-based synthetic approaches for the synthesis of hierarchically structured materials.

The key point that emerges from this investigation is that *it is not straightforward to synthesize siliceous zeolites from clear solutions with these SDAs under conditions where silicalite-1 forms in a matter of hours.* It is certainly possible that one can find conditions with these (or other) organocations that lead to all-silica zeolite formation at 368 K; however, our results clearly show that for these organocations it does not occur under conditions where silicalite-1 forms in a matter of hours. Our results suggest that the zeolite community should not generalize the results from the studies of silicalite-1 growth from clear solutions to other siliceous zeolites. While the differences between the silicalite-1 system on the systems investigated here could be simply due to differences in the kinetics of material formation (higher activation energies), the syntheses performed at elevated temperatures would seem to rule this out for the MTW case. The inability to grow MTW in the presence of seeds gives an additional credence to this, as the presence of the seed crystals should allow the uncoupling of the nucleation and growth process. However, even if it is as simple as differences in the activation energy for nucleation and growth, as one increases or changes the synthesis temperature the role and effect of various noncovalent forces such as electrostatics, hydrophobic hydration, and hydrogen bonding will change. This observation would lead to the conclusion that if weak forces are what lead to the rapid formation of silicalite-1 at 368 K, those forces are likely not relevant in conventional syntheses performed at 433 K, or in other words are not relevant for the synthesis of most siliceous zeolites.

Conclusions

This work has investigated the solution behavior of several TEOS/organocation/water solutions. All mixtures studied contain colloidal silica particles, the size and shape of which appear to depend on the organocation identity. However, none of the mixtures studied can direct the nucleation or growth of a zeolite phase, despite varying several parameters including changing organocation identity, hydroxide content, alkali content, synthesis temperature, ethanol content, and seeding. The inability to nucleate or crystallize a siliceous phase does not appear to be sensitive to whether the organocation is highly selective or nonselective. These results are dramatically different from what is observed in the TPA−silicalite-1 clear solution synthesis. This work raises the concern that the description of nucleation and growth developed from the clear solution synthesis of silicalite-1 may not be a general one, given our inability to synthesize any other siliceous zeolite phase under similar conditions. Current work is attempting to answer the following question: *why is the TPA−silicalite-1 system unique?* Progress will be reported elsewhere.

Acknowledgment. The authors acknowledge financial support from Texas A&M University. The SAXS instruments were purchased from funds obtained under NSF Grant CTS-0215838. The authors acknowledge the X-Ray Diffraction Facility at Texas A&M University for access to the XRD and SAXS instruments. The authors also gratefully acknowledge Dr. Abraham Clearfield for use of the TGA instrument. D.F.S. thanks J. S. Pedersen for useful discussions and R. F. Lobo for the copy of ref 49 before it was published.

Supporting Information Available: Autocorrelation functions of DLS measurements for sample 1TEOS:0.18**I**:20H_2O aged at room temperature for 24 h and heated at 368 K for 14 days; table summarizing TGA data; summary of SAXS fitting for sample 1TEOS:0.18**I**:20H_2O heated for 2 weeks at 368 K; TGA plots, SAXS data, and fitting for 1TEOS:0.18**I**:20H_2O

heated for 1 week at 368 K; PXRD patterns of high temperature syntheses of ZSM-12 and silicalite-1; PXRD patterns of syntheses performed in the presence of ZSM-12 seeds; plots showing the results of the SAXS full profile fitting for various particles geometries for the sample 1TEOS:0.18**I**:20H_2O heated for 2 weeks at 368 K; and size evolution of 1TEOS:0.36TPAOH:20H_2O heated at 368 K obtained by ex situ SAXS measurement. This material is available free of charge via the Internet at http://pubs.acs.org

References and Notes

(1) Barrer, R. M. *Hydrothermal Chemistry of Zeolites*; Academic Press: London, 1982.

(2) Breck, D. W. *Zeolite Molecular Sieves: Structure, Chemistry and Use*; Wiley: New York, 1974.

(3) Davis, M. E.; Lobo, R. F. *Chem. Mater.* **1992**, *4*, 756.

(4) Cundy, C. S.; Cox, P. A. *Chem. Rev.* **2003**, *103*, 663.

(5) Burkett, S. L.; Davis, M. E. *J. Phys. Chem.* **1994**, *98*, 4647.

(6) Burkett, S. L.; Davis, M. E. *Chem. Mater.* **1995**, *7*, 1453.

(7) Burkett, S. L.; Davis, M. E. *Chem. Mater.* **1995**, *7*, 920.

(8) Cundy, C. S.; Lowe, B. M.; Sinclair, D. M. *J. Cryst. Growth* **1990**, *100*, 189.

(9) de Moor, P.-P. E. A.; Beelen, T. P. M.; Komanschek, B. U.; Diat, O.; van Santen, R. A. *J. Phys. Chem. B* **1997**, *101*, 11077.

(10) de Moor, P.-P. E. A.; Beelen, T. P. M.; Komanschek, B. U.; van Santen, R. A. *Microporous Mesoporous Mater.* **1998**, *21*, 263.

(11) de Moor, P.-P. E. A.; Beelen, T. P. M.; van Santen, R. A. *Microporous Mater.* **1997**, *9*, 117.

(12) de Moor, P.-P. E. A.; Beelen, T. P. M.; van Santen, R. A. *J. Appl. Crystallogr.* **1997**, *30*, 675.

(13) de Moor, P.-P. E. A.; Beelen, T. P. M.; van Santen, R. A. *J. Phys. Chem. B* **1999**, *103*, 1639.

(14) de Moor, P.-P. E. A.; Beelen, T. P. M.; van Santen, R. A.; Beck, L. W.; Davis, M. E. *J. Phys. Chem. B* **2000**, *104*, 7600.

(15) de Moor, P.-P. E. A.; Beelen, T. P. M.; van Santen, R. A.; Tsuji, K.; Davis, M. E. *Chem. Mater.* **1999**, *11*, 36.

(16) Kubota, Y.; Helmkamp, M. M.; Zones, S. I.; Davis, M. E. *Microporous Mater.* **1996**, *6*, 213.

(17) Nakagawa, Y.; Lee, G. S.; Harris, T. V.; Yuen, L. T.; Zones, S. I. *Microporous Mesoporous Mater.* **1998**, *22*, 69.

(18) Gies, H.; Marler, B.; Werthmann, U. *Synthesis of Porosils: Crystalline Nanoporous Silicas with Cage- and Channel-Like Void Structures*; Springer: Berlin, 1998; Vol. 1.

(19) Lobo, R. F.; Zones, S. I.; Davis, M. E. *J. Inclusion Phenom. Mol. Recognit. Chem.* **1995**, *21*, 47.

(20) Wagner, P.; Nakagawa, Y.; Lee, G. S.; Davis, M. E.; Elomari, S.; Medrud, R. C.; Zones, S. I. *J. Am. Chem. Soc.* **2000**, *122*, 263.

(21) Watson, J. N.; Brown, A. S.; Iton, L. E.; White, J. W. *J. Chem. Soc., Faraday Trans.* **1998**, *94*, 2181.

(22) Watson, J. N.; Iton, L. E.; Keir, R. I.; Thomas, J. C.; Dowling, T. L.; White, J. W. *J. Phys. Chem. B* **1997**, *101*, 10094.

(23) Zones, S. I.; Nakagawa, Y.; Yuen, L. T.; Harris, T. V. *J. Am. Chem. Soc.* **1996**, *118*, 7558.

(24) Zones, S. I.; Nakagawa, Y.; Lee, G. S.; Chen, C. Y.; Yuen, L. T. *Microporous Mesoporous Mater.* **1998**, *21*, 199.

(25) Persson, A. E.; Schoeman, B. J.; Sterte, J.; Ottesstedt, J. E. *Zeolites* **1994**, *14*, 557.

(26) Schoeman, B. J. *Microporous Mesoporous Mater.* **1997**, *9*, 267.

(27) Schoeman, B. J. *Zeolites* **1997**, *18*, 97.

(28) Schoeman, B. J. *Stud. Surf. Sci. Catal.* **1997**, *105*, 647.

(29) Schoeman, B. J. *Microporous Mesoporous Mater.* **1998**, *22*, 9.

(30) Schoeman, B. J.; Regev, O. *Zeolites* **1996**, *17*, 447.

(31) Schoeman, B. J.; Sterte, J.; Otterstedt, J. E. *Zeolites* **1994**, *14*, 568.

(32) Kirschhock, C. E. A.; Buschmann, V.; Kremer, S.; Ravishankar, R.; Houssin, C. J. Y.; Mojet, B. L.; van Santen, R. A.; Grobet, P. J.; Jacobs, P. A.; Martens, J. A. *Angew. Chem., Int. Ed.* **2001**, *40*, 2637.

(33) Kirschhock, C. E. A.; Ravishankar, R.; Jacobs, P. A.; Martens, J. A. *J. Phys. Chem. B* **1999**, *103*, 11021.

(34) Kirschhock, C. E. A.; Ravishankar, R.; Van Looveren, L.; Jacobs, P. A.; Martens, J. A. *J. Phys. Chem. B* **1999**, *103*, 4972.

(35) Ravishankar, R.; Kirschhock, C. E. A.; Schoeman, B. J.; Vanoppen, P.; Grobet, P. J.; Storck, S.; Maier, W.; Martens, J. A.; De Schryver, F. C.; Jacobs, P. A. *J. Phys. Chem. B* **1998**, *102*, 2633.

(36) Ravishankar, R.; Kirschhock, C. E. A.; Verspeurt, F.; Grobet, P. J.; Jacobs, P. A.; Martens, J. A. *J. Phys. Chem. B* **1999**, *103*, 4965.

(37) Ravishankar, R.; Kirschhock, C. E. A.; Knops-Gerrits, P.-P.; Feijen, E. J. P.; Grobet, P. J.; Vanoppen, P.; De Schryver, F. C.; Miehe, G.; Fuess, H.; Schoeman, B. J.; Jacobs, P. A.; Martens, J. A. *J. Phys. Chem. B* **1999**, *103*, 4960.

(38) Mintova, S.; Olson, N. H.; Senker, J.; Bein, T. *Angew. Chem., Int. Ed.* **2002**, *41*, 2258.

(39) Mintova, S.; Valtchev, V. *Microporous Mesoporous Mater.* **2002**, *55*, 171.

(40) Mintova, S.; Valtchev, V.; Bein, T. *Colloids Surf. A* **2003**, *217*, 153.

(41) Kragten, D. D.; Fedeyko, J. M.; Sawant, K. R.; Rimer, J. D.; Vlachos, D. G.; Lobo, R. F.; Tsapatsis, M. *J. Phys. Chem. B* **2003**, *107*, 10006.

(42) Yang, S.; Navrotsky, A. *Chem. Mater.* **2002**, *14*, 2803.

(43) Yang, S.; Navrotsky, A.; Wesolowski, D.; Pople, J. A. *Chem. Mater.* **2004**, *16*, 210.

(44) Cundy, C. S.; Forrest, J. O.; Plaisted, R. J. *Microporous Mesoporous Mater.* **2003**, *66*, 143.

(45) Knight, C. T. G.; Kinrade, S. D. *J. Phys. Chem. B* **2002**, *106*, 3329.

(46) Kirschhock, C. E. A.; Ravishankar, R.; Verspeurt, F.; Grobet, P. J.; Jacobs, P. A.; Martens, J. A. *J. Phys. Chem. B* **2002**, *106*, 3333.

(47) Ramanan, H.; Kokkoli, E.; Tsapatsis, M. *Angew. Chem., Int. Ed.* **2004**, *43*, 4558.

(48) Kirschhock, C. E. A.; Liang, D.; Aerts, A.; Aerts, C. A.; Kremer, S. P. B.; Jacobs, P. A.; Van Tendeloo, G.; Martens, J. A. *Angew. Chem., Int. Ed.* **2004**, *43*, 4562.

(49) Fedeyko, J. M.; Rimer, J. D.; Lobo, R. F.; Vlachos, D. G. *J. Phys. Chem. B* **2004**, *108*, 12271

(50) Rosinski, E. J.; Rubin, M. K. U.S. Patent 3,832,449, 1974.

(51) Rubin, M. K. U.S. Patent 4,585,637, 1985.

(52) Rubin, M. K. U.S. Patent 4,636,373, 1987.

(53) Valyocsik, E. W. U.S. Patent 4,593,193, 1985.

(54) Bhaumik, A.; Dongare, M. K.; Kumar, R. *Microporous Mater.* **1995**, *5*, 173.

(55) Tsuji, K.; Davis, M. E. *Microporous Mater.* **1997**, *11*, 53.

(56) Camblor, M. A.; Villaescusa, L. A.; Díaz-Cabañas, M. J. *Top. Catal.* **1999**, *9*, 59.

(57) Goepper, M.; Li, H.-X.; Davis, M. E. *Chem. Commun.* **1992**, 1665.

(58) Mitra, A.; Kirby, C. W.; Wang, Z. B.; Huang, L. M.; Wang, H. T.; Huang, Y. N.; Yan, Y. S. *Microporous Mesoporous Mater.* **2002**, *54*, 175.

(59) Ritsch, S.; Ohnishi, N.; Ohsuna, T.; Hiraga, K.; Terasaki, O.; Kubota, Y.; Sugi, Y. *Chem. Mater.* **1998**, *10*, 3958.

(60) Shantz, D. F.; Fild, C.; Koller, H.; Lobo, R. F. *J. Phys. Chem. B* **1999**, *103*, 10858.

(61) Shantz, D. F.; Lobo, R. F. *Chem. Mater.* **1998**, *10*, 4015.

(62) Terasaki, O.; Ohsuna, T.; Sakuma, H.; Watanabe, D.; Nakagawa, Y.; Medrud, R. C. *Chem. Mater.* **1996**, *8*, 463.

(63) Dahneke, B. E. *Measurement of Suspended Particles by Quasi-Elastic Light Scattering*; Wiley: New York, 1983.

(64) Svergun, D. I. *J. Appl. Crystallogr.* **1992**, *25*, 495.

(65) Glatter, O. *J. Appl. Crystallogr.* **1977**, *10*, 415.

(66) Glatter, O. *J. Appl. Crystallogr.* **1979**, *12*, 166.

(67) Glatter, O. *J. Appl. Crystallogr.* **1980**, *13*, 7.

(68) Glatter, O. *J. Appl. Crystallogr.* **1980**, *13*, 577.

(69) Pedersen, J. S. *Adv. Colloid Interface Sci.* **1997**, *70*, 171.

(70) Gapal, S.; Yoo, K.; Smirniotis, P. G. *Microporous Mesoporous Mater.* **2001**, *49*, 149.

(71) Glatter, O.; Kratky, O. *Small Angle X-Ray Scattering*; Academic Press: London, 1982.

(72) Guinier, A.; Fournet, G. *Small-Angle Scattering of X-Rays*; John Wiley & Sons: New York, 1955.

(73) Koller, H.; Lobo, R. F.; Burkett, S. L.; Davis, M. E. *J. Phys. Chem.* **1995**, *99*, 12588.

(74) Jacobs, P. A.; Derouane, E. G.; Weitkamp, J. *J. Chem. Soc., Chem. Commun.* **1981**, 591.

(75) Coudurier, G.; Naccache, C.; Vedrine, J. C. *J. Chem. Soc., Chem. Commun.* **1982**, 1413.

(76) Gonthier, S.; Thompson, R. W. *Stud. Surf. Sci. Catal.* **1994**, *85*, 43.

(77) Shantz, D. F.; Schmedt auf der Günne, J.; Koller, H.; Lobo, R. F. *J. Am. Chem. Soc.* **2000**, *122*, 6659.

(78) Nakagawa, Y. WO Patent 95 09812, 1995.

(79) Iler, R. K. *The Chemistry of Silica: solubility, polymerization, colloid and surface properties and biochemistry*; Wiley: New York, 1979.